THE POISSON LINE AS A STRAIGHT LINE REFERENCE

LEE V. GRIFFITH

Lawrence Livermore National Laboratory

Livermore, CA.

Summary

The Poisson Alignment Reference (PAR) system was developed in response to the need for a highly accurate linear reference that could operate as an element in a "real time" alignment feedback loop. The system will (or at least is expected to) provide transverse positional data on approximately 60 targets distributed over 300 m, with an accuracy of better than 25 μm. The PAR system employs a large diameter (46-cm-diam for 60 targets) collimated laser beam. The beam must be propagated in a vacuum, to avoid refractive bending. The stability of the beam is guaranteed via a high bandwidth feedback loop, that maintains beam pointing within 5 μm over 300 m. Resolution of target position within the large laser beam is achieved by employing the Poisson spot formed in the shadow of spheres (the targets) in the beam. The Poisson spot from a 2.5-cm-diameter sphere in a HeNe beam is approximately 8-mm in diameter at 300 m, and its center can be resolved to about 2-3 μm using a photo-electric quadrant detector. Much of the advantage of this system resides in the fact that the targets can remain in place at all times, there are no radiation sensitive detectors employed along the alignment axis, and the targets are extremely simple. This paper describes, in some detail, the mathematical modeling of the refractive effects common to all optical alignment systems. The paper continues to describes the Poisson spot and the conceptual design for employing the PAR system in accelerator and free electron laser (wiggler) alignment.

Propagating a Laser Beam

Refractive Effects

The principal feature of an alignment system is a straight line reference, or SLR. It would be inconceivable to make a mechanical SLR to the tolerances needed for an FEL. Lasers form what is generally considered a straight line, but as is shown in Eq. (6), this is not true in air. The beam will bend in the atmosphere from changes in the refractive index. The refractive index is sensitive to both temperature and pressure variations. Some perspective on the atmospheric bending effect on light is provided in Ref. 5. If one were to use the SLAC approach, a deviation from a straight line path can be calculated from the following considerations: if only deviations in the vertical direction are considered, the refractive index can be written as

$$n(y) = n_o(1 - \varepsilon y) , \tag{3}$$

where $n(y)$ is the index of refraction as a function of the vertical position y and $n_o\varepsilon$ is the gradient in the vertical direction. The vector form of the differential equation of a light ray is

$$d/ds\,(n\,d\mathbf{r}/ds) = \text{grad}\ n \ , \tag{4}$$

where $\mathbf{r} = \mathbf{j}y + \mathbf{k}z$; $\mathbf{j}$ and $\mathbf{k}$ are the unit vectors in the y and z directions, respectively; and s is the distance along the ray. To a very good approximation, $s = z$; thus Eq. (4) can be reduced to

$$d/dz\,(n\,dy/dz) = -n_o\varepsilon \ . \tag{5}$$

For a paraxial ray starting on the axis, where $n = n_o$, the solution to Eq. (5) is

$$y = -\varepsilon z^2/2 \ . \tag{6}$$

The problem is to find ε, which can be derived by starting with the Lorentz-Lorentz formula[5,15]:

$$A = (RT/p)\,(n^2 - 1)/3 \ , \tag{7}$$

where A is the molar refractivity, R is the gas constant, T is the temperature, and p is the pressure. Equation (7) can be rearranged as

$$n - 1 = \frac{3A\,p}{[RT(n + 1)]} , \tag{8}$$

and noting that $n + 1 \cong 2$:

$$n - 1 \cong \frac{3A(p/T)}{2R} \ . \tag{9}$$

At standard temperature and pressure (298 K and 760 Torr), $n - 1 = 3 \times 10^{-4}$; thus $3A/(2R)$ is equal to 1.2×10^{-4} K/Torr. Pressure and temperature can be expressed as a function of y, to the first order, as

$$p(y) = p_o + (dp/dy)y = p_o + p'\,y , \tag{10}$$

and

$$T(y) = T_o + (dT/dy)y = T_o + T'\,y \ . \tag{11}$$

If the ratio $p(y)/T(y)$ is expanded in a Taylor series about $y_o = 0$, then

$$p(y)/T(y) = p_o/T_o + p'y/T_o - p_oT'y/T_o^2 + (\text{higher order terms}) \ , \tag{12}$$

where p_o and T_o are the nominal pressure and temperature in the line of sight at y_o. Now substituting for n,

$$n(y) = n_o - \varepsilon y \tag{13}$$

yields

$$n_o - n_o\,\varepsilon\,y - 1 = \frac{3A}{2R}\left(\frac{p_o}{T_o} + \frac{p'y}{T_o} - \frac{p_oT'y}{T_0^2}\right) , \tag{14}$$

At $y = 0$,

$$n_o - 1 = \frac{3A(p_o/T_o)}{2R} = 1.2 \times 10^{-4}\,p_o/T_o \ ; \tag{15}$$

thus

$$n_o\,\varepsilon = 1.2 \times 10^{-4}\ \text{K/Torr}\left(\frac{p_o\,T'}{T_o^2} - \frac{p'}{T_o}\right) . \tag{16}$$

The value of n_o is 1.0003 and the pressure and temperature (p_o and T_o) are in Torr and Kelvin. The pressure gradient, p', is $-1.15 \times 10^{-4}\,p_o/m$ (for

air) and is generally a minor contributor to refractive bending. However, a temperature gradient as small as 1 K/m would bend the beam 4.5 mm over a 300-m path. To keep the refractive bending from the temperature gradient (T) at tolerable levels, the pressure (p_o) should be below 10^{-3} Torr. The maximum allowable pressure in the propagation path depends on the allowable uncertainty in the straightness of the laser beam, the length of the path, and how well temperature gradients can be controlled.

Divergence

If a Gaussian laser beam is used as an alignment reference, the ability to resolve the location of the beam is proportional to the beam radius. However, due to divergence, the beam radius increases with propagation distance. To keep the beam radius minimized over the entire propagation path, it is necessary to focus the beam to a waist at the midpoint. The equation for the beam waist, w_o, for a given beam radius, $w(z)$, is[16]

$$w_o^2 = \frac{w^2 \pm \left[w^4 - \left(\frac{2\lambda z}{\pi}\right)^2\right]^{0.5}}{2}, \qquad (17)$$

where z is the distance between the waist and the observation plane. If a 5-mm radius beam is required at a distance of 150 m (one half the total propagation distance), then there is no real solution for w_o (assuming λ = 488 or 632 nm). Therefore, a Gaussian beam is less suitable for the SLR than the Poisson line.

The Poisson Line

The key element of any alignment scheme is the SLR[5,10,13,14] The Poisson line is one method of generating this line by diffraction. When an opaque sphere is illuminated by a plane wave, as shown in Fig. 2, a diffraction pattern that has the following characteristics is formed behind the sphere:

- There is a line of light, the Poisson line, generated behind the sphere. This line is perpendicular to the incident plane wave and, if extended backwards, passes through the center of the sphere.

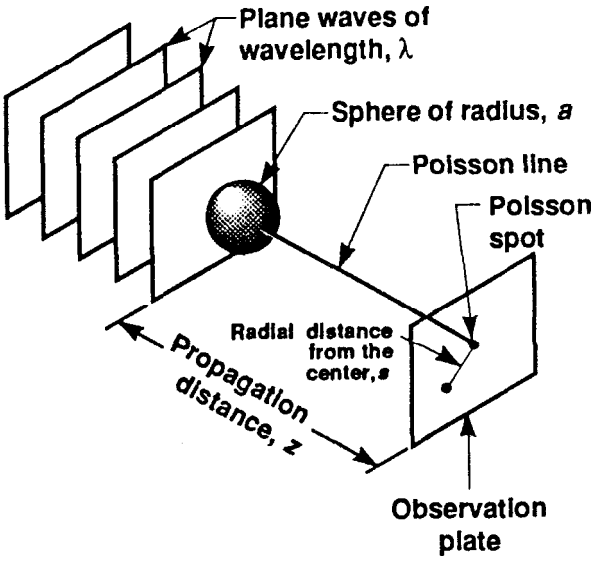

Figure 2 A sphere illuminated by a laser will produce a line of light (the Poisson line) in the shadow of the sphere. The intersection of the Poisson line with an observation plane identifies the sphere location relative to the laser beam or other spheres in the beam.

- The intensity of the line increases asymptotically to the incident intensity as distance from the sphere increases.
- The diameter of the line decreases as the diameter of the sphere increases.
- The diameter of the line increases for increasing distances from the sphere; however, the diameter of the line over any distance behind the sphere can always be kept smaller than a Gaussian beam propagating over the same distance.

The diffraction pattern can be observed by placing an observation screen or camera perpendicular to the Poisson line at any plane behind the sphere. Typical diffraction patterns are shown in Figs. 3(a) and (b). These photographs were taken with a Graflex camera that allows the light to be directly imposed on the film. The diffraction pattern was formed by a 12.7-mm-radius sphere, which was 50 m from the observation plane in Fig. 3(a) and 100 m from the observation plane in Fig. 3(b). The bright area around the shadow of the sphere is part of the 150-mm-diam incident laser beam. The central bright area in the shadow is the Poisson spot, which is the intersection of the Poisson line and

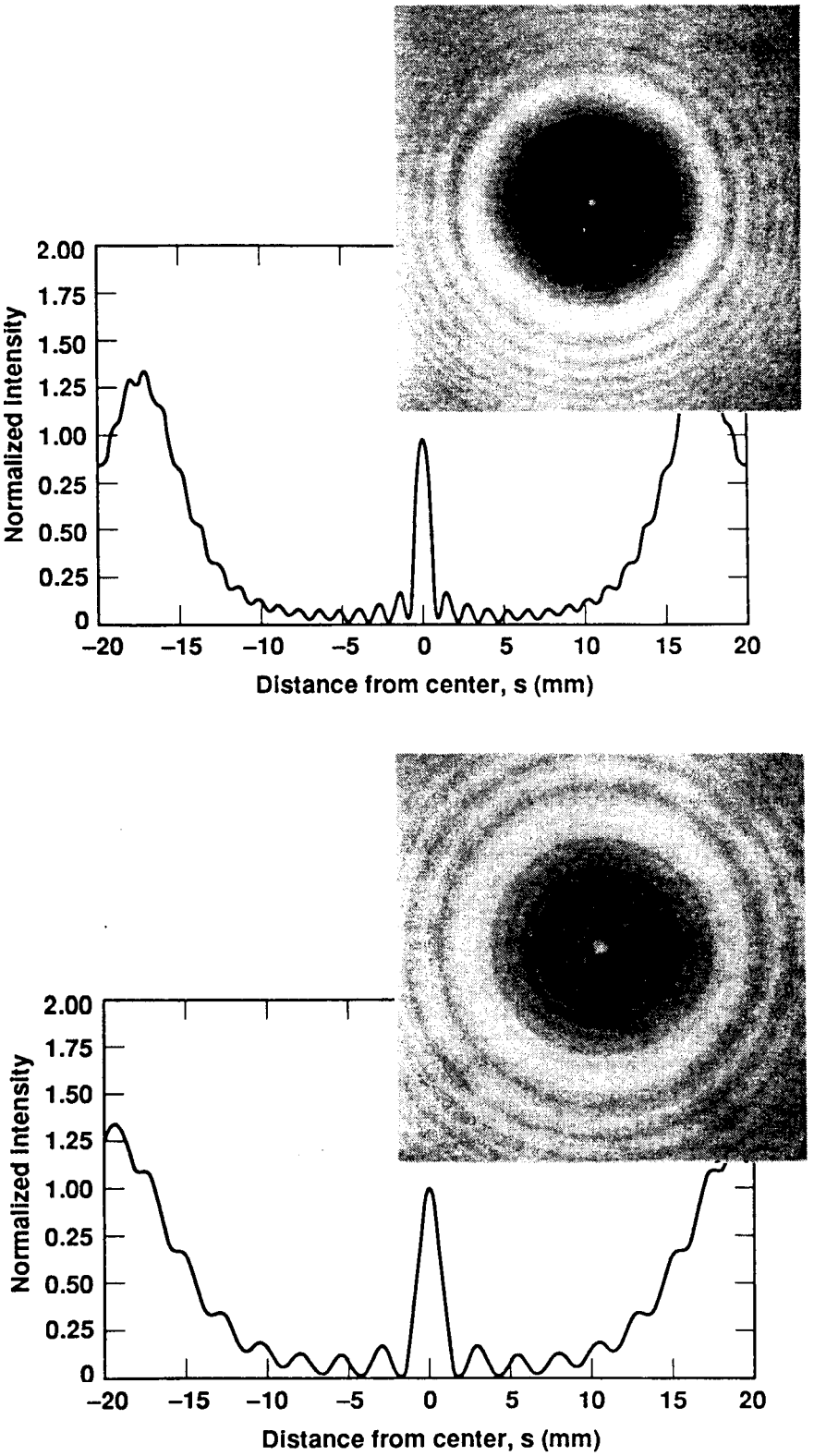

Figure 3. These photos show the Poisson spot from a 25-mm-diam sphere in an observation plane at (a) 50 m and (b) 100 m. The associated plots are the calculated intensity profiles out to the edge of the shadow.

the observation plane. The intensity, I, of the diffraction pattern is given by[17]

$$I(s) = 1 - 4(\pi u)^{0.5}(S_1 \sin\alpha + S_2 \cos\alpha) + 4\pi u(S_1^2 + S_2^2) , \quad (18)$$

where s is the radial distance from the center of the Poisson spot, S_1 and S_2 are summations of Bessel functions given by

$$S_1 = \sum_{n=0}^{\infty} (4n+1)(-1)^n J_{2n+1/2}(u/2) J_{4n+1}(v)/v , \quad (19)$$

and

$$S_2 = \sum_{n=0}^{\infty} (4n+3)(-1)^{n+1} J_{2n+3/2}(u/2) J_{4n+3}(v)/v , \quad (20)$$

where

$$u = ka^2/2z , \quad (21)$$
$$v = ksa/z , \quad (22)$$
$$\alpha = ks^2/2z + u/2 . \quad (23)$$

In Eqs. (18)-(23) a is the radius of the sphere, λ is the laser wavelength, and k is the propagation number $2\pi/\lambda$. Figures 4(a) and (b) show the calculated intensity, $I(s)$, for the Poisson spot of a 6.35-mm-diam sphere 26.5 m from the observation plane and of a 25.4-mm-diam sphere 300 m from the observation plane, respectively.

The Poisson line generated as described above only passes through one fixed point, the center of the sphere. To serve as a reference line, the Poisson line must be constrained to pass through a second fixed point. The center of a quad-cell (quadrant detector) serves as the second fixed point. By centering the Poisson spot on the quad-cell, using a feedback circuit between the quad-cell and a mirror that actively steers the incident plane wave, one forms the Poisson reference line, which is ostensibly as stable as the two fixed points.

Since there is a significant amount of energy in the rings around the bright central spot, an aperture over the quad-cell should be sized to match the first dark ring. The quad-cell determines the location of the mean of the energy in the Poisson spot relative to the center. Let A, B, C, and D represent the sum of the energy in each quadrant; then the offset from center can be expressed as

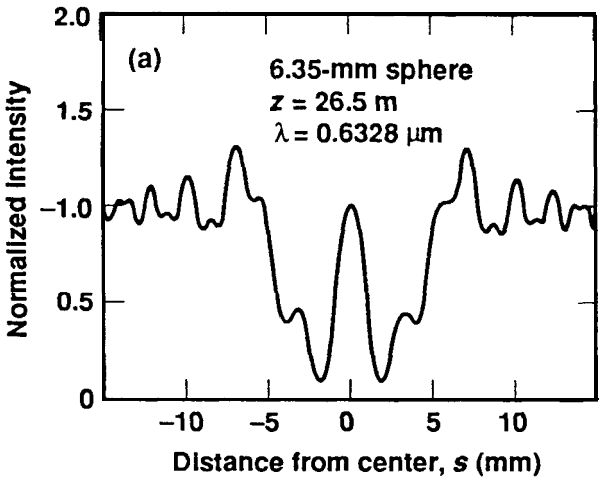

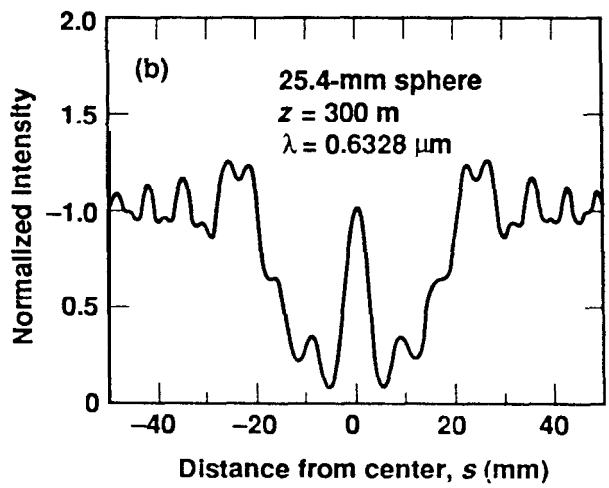

Figure 4. A 635-mm sphere (a) was used in a 26.5-m test to simulate the effects of a 25.4-mm sphere (b) 300 m from the observation plane.

$$\delta x = K[(A + D) - (B + C)] \quad (24)$$

and

$$\delta y = K[(A + B) - (C + D)] . \quad (25)$$

where A, B, C, and D are the currents from each quadrant, as illustrated:

K is a proportionality constant to convert the quad-cell current output to a linear dimension. Figure 5 is a calibration curve that shows that K is quite linear through a region near the center. Although quad-cells can be used for measuring offsets, they are generally better as nulling or centering devices. The curve eventually changes direction because the quad-cell has been moved more than the width of the first dark ring. This causes part of the central bright spot to be masked by the aperture, while on the opposite side of the quad-cell, energy is starting to be added by the first bright ring. It is also important to note that quad-cell output indicates location of the mean of the energy. From a computational standpoint, it is important to distinguish the location of the mean of the energy from the centroid of the energy.

There are major advantages to placing several spheres in a very large diameter beam simultaneously, as discussed in the next section. When there are two (or more) spheres in the collimated laser beam, there is some degree of mutual influence of one sphere on the diffraction pattern of an adjacent sphere. The symmetry of the diffraction pattern is altered, causing a shift of the center of energy of the Poisson spot. Figure 6 illustrates the pertinent dimensions in calculating the offset of a Poisson spot as a result of diffraction from an ad' cent sphere. The intensity at a point P is[17]

$$\begin{aligned} I(s_1,\theta) &= 1 - 4(\pi u_1)^{0.5}\,(S_{11}\sin\alpha_1 + S_{21}\cos\alpha_1) \\ &\quad - 4(\pi u_2)^{0.5}\,(S_{12}\sin\alpha_2 + S_{22}\cos\alpha_2) \\ &\quad + 4\pi u_1(S_{11}^2 + S_{21}^2) + 4\pi u_2(S_{12}^2 \\ &\quad + S_{22}^2) + 8\pi(u_1u_2)^{0.5} \\ &\quad \times \{\cos(\alpha_2-\alpha_1)[S_{11}S_{12} + S_{21}S_{22}] \\ &\quad + \sin(\alpha_2-\alpha_1)\,[S_{12}\,S_{21} - S_{11}S_{22}]\}\ . \end{aligned} \tag{26}$$

The arguments of this function are defined in Eqs. (27)-(32), where i = 1,2 identifies the sphere.

$$\alpha_i = ks_i^2/2z + u_i/2\ , \tag{27}$$

$$S_{1i} = \sum_{n=0}^{\infty}(4n+1)(-1)^n\,J_{2n+1/2}(u_i/2) \times J_{4n+1}(v_i)/v_i\ , \tag{28}$$

$$S_{2i} = \sum_{n=0}(4n+3)(-1)^{n+1}\,J_{2n+3/2}(u_i/2) \times J_{4n+3}(v_i)/v_i\ , \tag{29}$$

$$u_i = k\,a_i^2/2z\ , \tag{30}$$

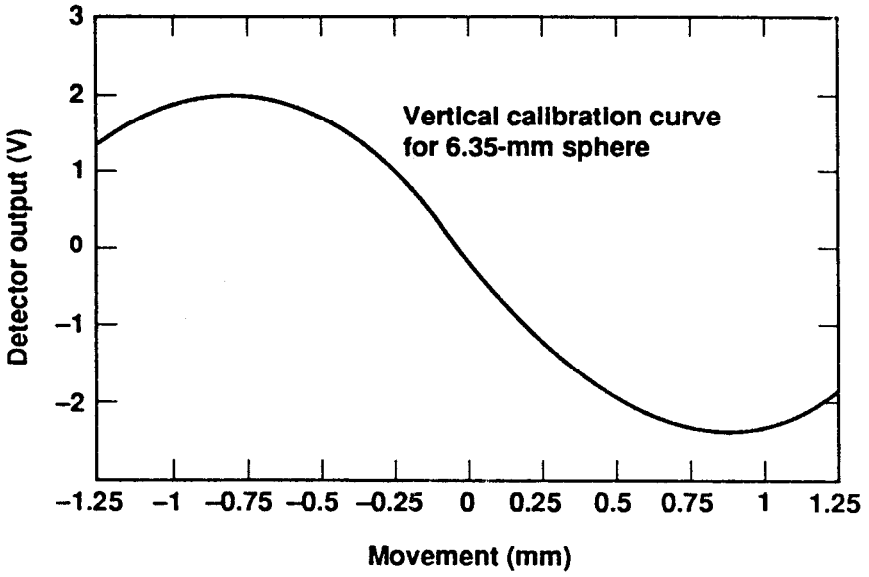

Figure 5. Quad-cell calibration curves are influenced by beam intensity and might be distorted by stray light.

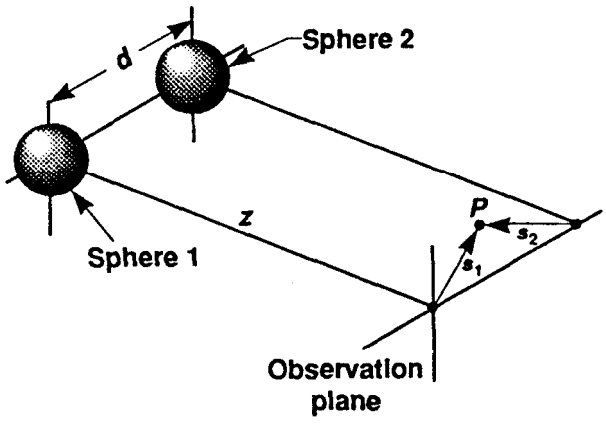

$z \equiv$ Distances from spheres to observation plane

$P \equiv$ Point in the observation plane

$s_1, s_2 \equiv$ Radial distance from the Center of the Poisson spots to the point p

Figure 6. Diffraction from two adjacent spheres will interact. The separation of the spheres (d) must be about 25 mm edge-to-edge to assure an acceptably small shift in Poisson spot in the observation plane. Z is the distance from the spheres to the observation plane; P is a point in the observation plane; and s_1 and s_2 are radial distances from the center of the Poisson spots to the point P.

$$v_i = k s_i a_i / z \ , \tag{31}$$

and, as before,

$$k = 2\pi/\lambda \ . \tag{32}$$

In Eqs. (26)-(32), a_i is the radius of the sphere i, z is the propagation length between the spheres and the observation plane, and λ is the laser wavelength. Techniques for solving the fractional-order Bessel functions can be found in *Handbook* of *Mathematical Functions.*[18] The value of s_2 is easily found from the cosine law

$$s_2 = (s_1^2 + d^2 - 2d\, s_1 \cos\theta)^{0.5} \ , \tag{33}$$

where s_1 and θ are the coordinates of the point P. Point P is the spot in the observation plane where the intensity is being calculated. Distance d is the center-to-center separation between the spheres.

Figure 7 shows the experimentally determined shift of a Poisson spot, from a stationary 6.35-mm-diam sphere, as a matching sphere moves toward it. The abscissa shows the center-to-center displacement of the spheres, and the ordinate shows the displacement of the midpoint of the energy distribution of the Poisson spot from the stationary sphere. The moving sphere is aligned such that its axis of motion will cause it to overlap the stationary sphere. The quad-cell that is monitoring the Poisson spot

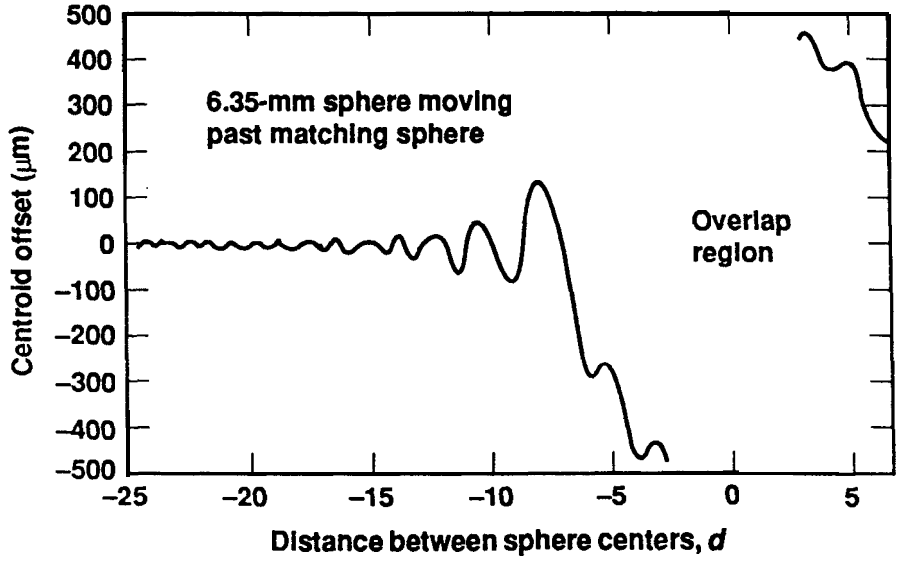

Figure 7. The center of a Poisson spot will move in an oscillatory manner as another sphere is moved toward the sphere creating the Poisson spot.

of the stationary sphere is on a calibrated stage that moves parallel to the moving sphere.

Two spheres were placed on the inlet window of the vacuum pipe as shown in the experimental setup (Fig. 8). A third sphere was attached to a ring on a calibrated stage. This third sphere, or probe sphere, could be moved vertically past a stationary sphere on the inlet window. The Poisson spot of the stationary sphere was centered on a quad-cell at the far end of the vacuum pipe, 26.5 m away. As the moving sphere was moved toward, over, and beyond the stationary sphere, the quad-cell was moved to keep the Poisson spot centered. Figure 7 shows the necessary displacement of the quad-cell as a function of sphere separation. The diffraction rings from the moving sphere have little effect on the stationary (measurement) sphere when the center-to-center separation is greater than about 20 mm.

The control sphere on the inlet window created a Poisson spot on a quad-cell in the closed-loop control system. This sphere was placed far enough away from the probe sphere that the two Poisson spots would not significantly interact.

The FEL might require a 300-m SLR. Calculations based on the equations above show that, at 300 m, 25-mm-diam spheres separated by 50 mm would produce no more than 10 μm of disturbance (error) in the Poisson spot of an adjacent sphere.

In the experimental setup to verify Eq. (26), it would have been possible to support the spheres on a glass plate perpendicular to the laser beam. However, in an FEL, there might be sufficiently high radiation levels to darken the glass; therefore, the spheres were supported on thin (25 or 50 μm), taut wires. Figures 9(a) and (b) show the effects of moving a 25-μm and a 50-μm wire past a 6.35-mm sphere. Note that if the wire is more than about 10 mm from the edge of the sphere, the wire's movement has a reasonably small influence on the apparent position of the sphere's Poisson spot. More important, once the wire moved between the edges of the sphere, the wire effects were less than 5 μm for any of the wires we tested.

There are a number of ways to attach the spheres to the wire. Holes of 250 μm have been electron-discharge machined into the spheres, and the wires have been laser welded into the holes. This technique has the advantage that there is no cantilevered load on the wire, but the machining and laser welding are expensive. Another method that has worked well is to machine-off two parallel flat surfaces (as in Fig. 21). Now, the wires can be contact welded

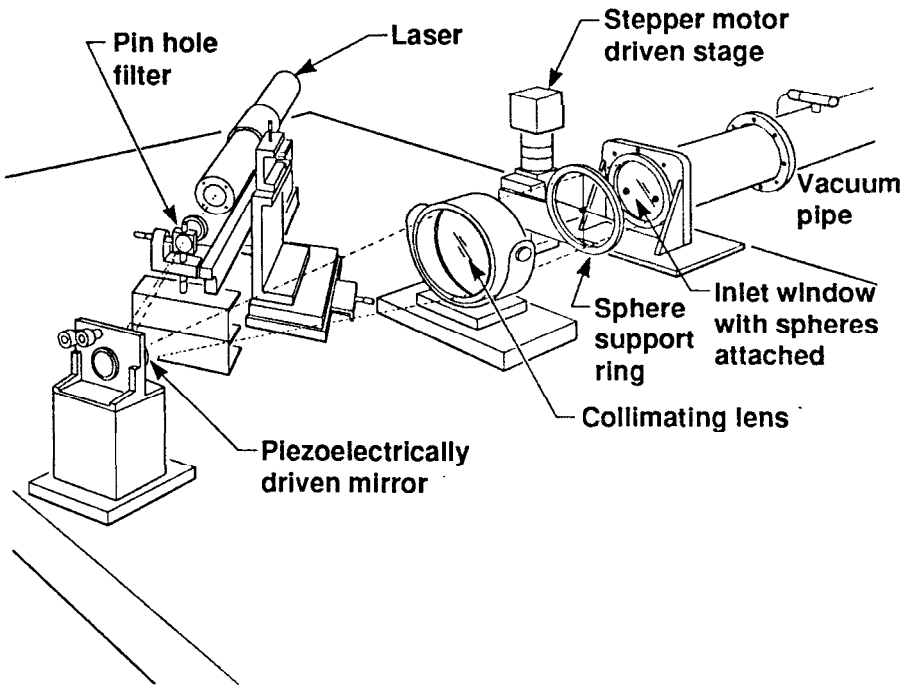

Figure 8. Experimental setup to measure diffraction interference effects.

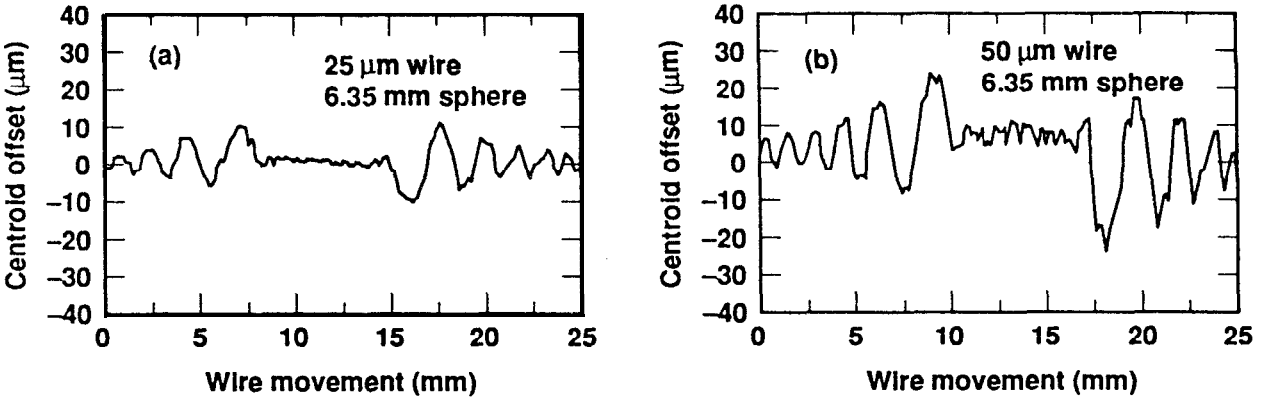

Figure 9. The alignment fiducials (spheres) can be supported on wires. Diffraction from wires of adjacent spheres will cause the Poisson spot of a given sphere to move in an oscillatory manner, as indicated by moving a wire past a 6.35-mm sphere and observing the movement of the Poisson spot at 26.5 m; (a) 25-μm wire and (b) 50-μm wire.

into place on one of the flat surfaces. Although there is clearly some movement on the wires, it has not resulted in vibrations that could be sensed on the quad-cells. Using a section of a sphere rather than a disk eliminates the need for tight tolerances on the pitch and yaw of the target support.

The Alignment Concept

To develop an understanding of how the Poisson spots can be used to align something, consider the following simplified case. Imagine that we want to align five magnets. For the moment, assume that we know exactly where the magnets are relative to a sphere that is attached to a perfectly transparent support. The laser beam and Poisson line in Fig. 10(a) will be the reference axis for the five magnets. The reference sphere and the center of the detector are the two fixed points necessary to define a straight line. Note that the laser beam can be translated in x and y, but not tilted, without changing the location of the Poisson spot on the detector. The fact that the laser beam can be translated emphasizes that the reference sphere and the quad-cell position detector are defining the line. By removing the reference sphere, we begin the alignment process by placing the sphere associated with the first magnet in the beam. As this sphere is moved up, down, and sideways in the beam, the Poisson spot it produces in the observation plane can be centered on the detector. The attachment of the sphere to the magnet must assure that the two move in unison and that there is no pitch or roll. Now, by holding the first magnet in place and removing the sphere, the next magnet [Fig. 10] can be aligned by placing its sphere in the beam and moving it until the Poisson spot it produces is centered on the detector. This process can be repeated until all five magnets are aligned.

What would happen, in the example above, if the laser beam started to drift, i.e., tilt, during the alignment process? Typical alignment lasers have stability specifications of 10^{-5} of 10^{-4} rad/hr. The reference sphere would have to be reinserted to detect the problem. The alignment of some of the magnets would have to be rechecked to assure that they were not aligned while the beam was tilted, or alternatively the reference sphere could be inserted before and after each magnet was aligned. Only a small part (say 10 μm) of the total alignment budget can be allocated to beam pointing in an FEL alignment system. A 10-μm laser pointing error would occur every 12 s (at 300 m) if the beam drifted at a linear rate of 10^{-5} rad/hr. However, laser drift can

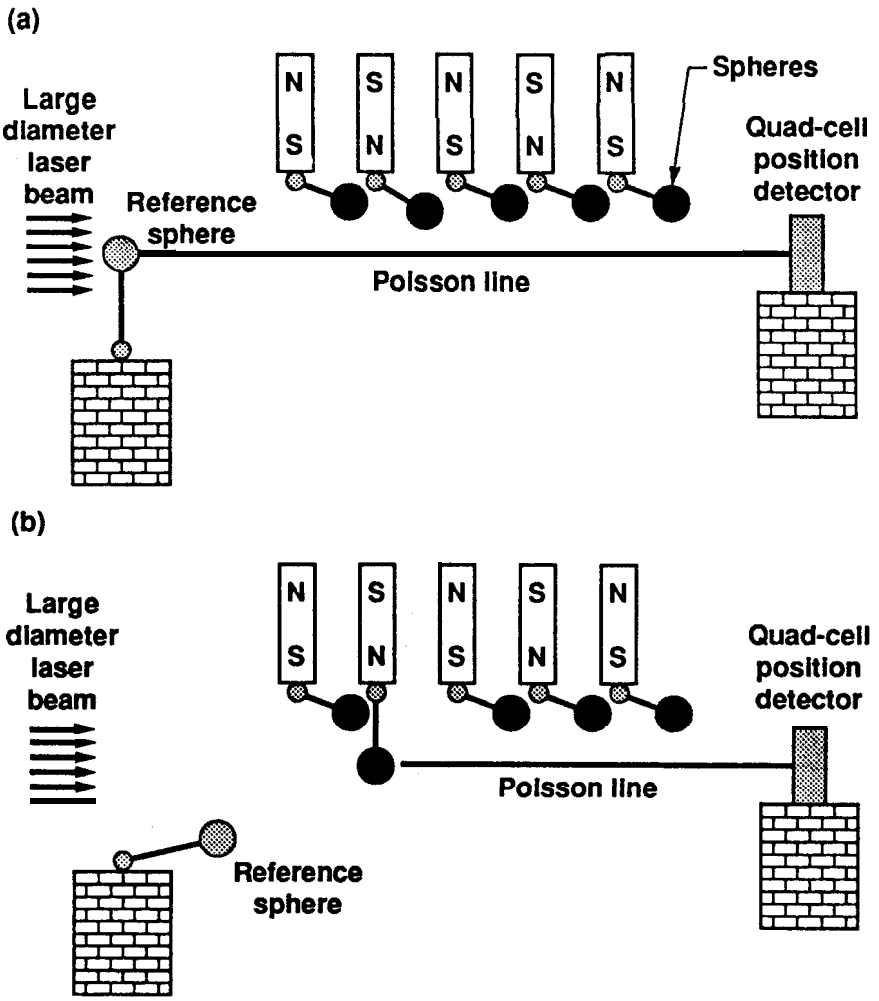

Figure 10. Magnets can be aligned by aligning the spherical fiducials, which are much more readily identified than magnetic centerlines; (a) establish a reference line and (b) move magnets so their fiducials fall on the reference line.

be more than adequately controlled with a closed loop feedback system if the reference sphere can be left in place.

Simultaneous alignment of many points in the FEL and continuous monitoring of beam pointing are essential because of ground motions and vibrations. Ground motion can be expected in response to a changing water table, post construction settling, nearby construction, and ground faults. Vibrations cover a frequency spectrum from thousandths of Hertz to thousands of Hertz. Earth tides, with a period of 94 min, are as much as 300 mm in amplitude[19] but the long wavelength results in negligible bending over the length of an FEL. Settling of the building and seismic activity are of much greater concern. The SLAC has been observed to move several millimeters each year, and typical construction practices indicate an expected settling of as much as 50 mm/yr. Even if this settling occurred linearly in time, the FEL would need to be realigned every 2-4 hrs. However, the difficulties that ground motion introduces for alignment are overwhelmed by the transient effects of internal heating during operation of the FEL. Internal heating is expected to necessitate realignment of the entire FEL every 10 seconds.

The alignment laser is particularly sensitive to vibrations since its pointing needs to be controlled to about 20 nrad. The laser and coilimator should be mounted on a table with a high level of internal damping. The collimator pointing system will actively damp vibrations below about 300 Hz (bandwidths over 1000 Hz

should be possible). The high bandwidth of the active control loop is largely due to the low moment of inertia of the beam-directing mirror, schematically illustrated in Fig. 11. Fractional gain in the pointing resolution of the piezoelcctrically driven mirror mount is achieved by adjusting the separation between the mirror and the pin hole. If the resolution of the mirror mount is θ_m, then the beam pointing resolution for small angles is[20]

$$\theta_p = 2L\theta_m/f \ , \tag{34}$$

where L is the distance from the pin hole to the mirror and f is the focal length of the collimating lens.

The reference sphere is to be kept in place at all times with a large-diameter laser beam. With some ingenuity, the spheres associated with ail the magnets could also be in the beam simultaneously. Leaving the spheres in place would eliminate several problems including, but not limited to, the repositioning error for the target inserter, high cost and poor reliability of the sphere insertion and retraction mechanism, and the low speed with which the magnets could be aligned or checked for alignment.

The reference sphere and all the other spheres can be in a single, large-diameter laser beam if an array of detectors is used as the second fixed point in defining a straight line. Each detector in the array would be given a specific x–y coordinate, and the sphere associated with each magnet would be offset to correspond with a particular detector, as shown in Fig. 12. Errors due to divergence of a large-diameter beam can be shown to be negligible. The radius of a beam is[16]

$$w(z) = w_o [1 + (z/z_R)^2]^{0.5} \ , \tag{35}$$

where w_o is the waist radius at $z = 0$ and z_R is the Rayieigh range

$$z_R = \pi w_o^2/\lambda \ . \tag{36}$$

In a large diameter diverging laser beam, a point that is a, off axis at $z = 0$ will move further off axis. At some distance z, this would produce an error

$$a(z) - a_o = a_o \{[1 + (z/z_R)^2]^{0.5} - 1\} \ . \tag{37}$$

The Rayleigh range, z_R, of a 0.4-m-diam helium-neon laser beam is 198 km; thus the term $\{[1 + (z/z_R)^2]^{0.5} - 1\}$ is 1.1 x 10^{6} at z = 300 m. Since the maximum a, in this beam is 0.2 m, the error due to divergence is less than 2.3 x 10^{-7} m for any sphere in the beam.

Several detector arrays can be made identically by calibrating each against a quasi-Hartmann plate. This Hartmann plate will be made from a glass plate with an array of spheres attached to one surface. The centers of the spheres will be arranged to match the desired array spacing. The size of the sphere will vary so that when the array is placed perpendicular to a laser beam, the resulting Poisson spots will match the Poisson spots of spheres distributed along a 300-m SLR.

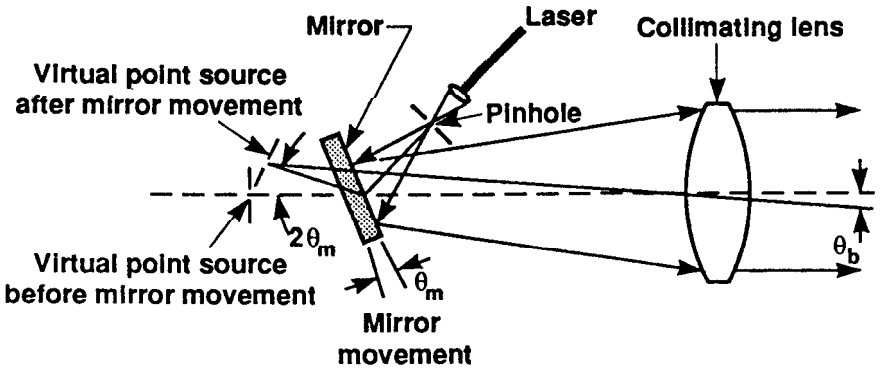

Figure 11. The folded collimator provides fractional gain in the beam-pointing resolution of the mirror mount.

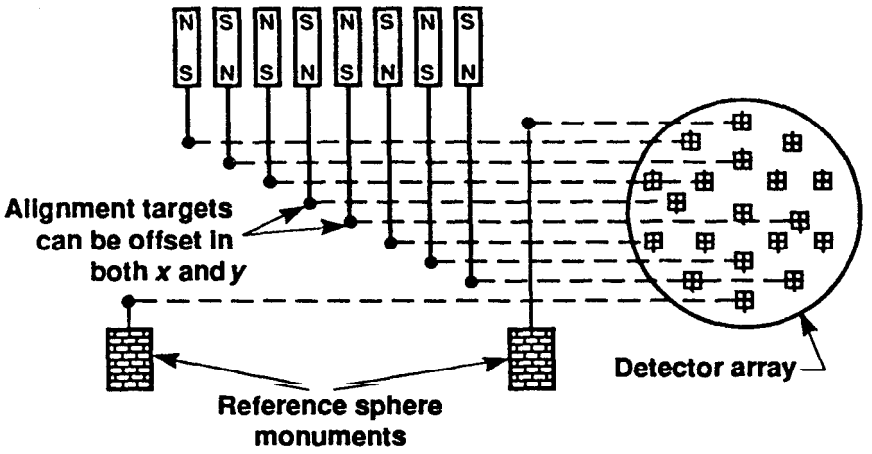

Figure 12. Many points along a magnetic axis can be monitored for alignment simultaneously by offsetting the targets in a large-diameter laser beam.